

## Physical characteristics of Eurasian winter temperature variability

This content has been downloaded from IOPscience. Please scroll down to see the full text.

2016 Environ. Res. Lett. 11 044009

(<http://iopscience.iop.org/1748-9326/11/4/044009>)

View [the table of contents for this issue](#), or go to the [journal homepage](#) for more

Download details:

IP Address: 210.77.64.105

This content was downloaded on 31/03/2017 at 11:12

Please note that [terms and conditions apply](#).

You may also be interested in:

[How does the SST variability over the western North Atlantic Ocean control Arctic warming over the Barents–Kara Seas?](#)

Ok Jung, Mi-Kyung Sung, Kazutoshi Sato et al.

[Influence of the Gulf Stream on the Barents Sea ice retreat and Eurasian coldness during early winter](#)

Kazutoshi Sato, Jun Inoue and Masahiro Watanabe

[Importance of combined winter and summer Arctic Oscillation \(AO\) on september sea ice extent](#)

Masayo Ogi, Søren Rysgaard and David G Barber

[Less winter cloud aids summer 2013 Arctic sea ice return from 2012 minimum](#)

Yinghui Liu and Jeffrey R Key

[Summertime atmosphere–ocean preconditionings for the Bering Sea ice retreat and the following severe winters in North America](#)

Takuya Nakanowatari, Jun Inoue, Kazutoshi Sato et al.

[Forcing of the wintertime atmospheric circulation by the multidecadal fluctuations of the North Atlantic ocean](#)

Yannick Peings and Gudrun Magnusdottir

[Atmospheric summer teleconnections and Greenland Ice Sheet surface mass variations: insights from MERRA-2](#)

Young-Kwon Lim, Siegfried D Schubert, Sophie M J Nowicki et al.

[Arctic moisture source for Eurasian snow cover variations in autumn](#)

Martin Wegmann, Yvan Orsolini, Marta Vázquez et al.

## Environmental Research Letters



## LETTER

## Physical characteristics of Eurasian winter temperature variability

## OPEN ACCESS

RECEIVED  
19 November 2015

REVISED  
7 March 2016

ACCEPTED FOR PUBLICATION  
15 March 2016

PUBLISHED  
7 April 2016

Original content from this work may be used under the terms of the [Creative Commons Attribution 3.0 licence](#).

Any further distribution of this work must maintain attribution to the author(s) and the title of the work, journal citation and DOI.



Kwang-Yul Kim and Seok-Woo Son

School of Earth and Environmental Sciences, Seoul National University, 1 Gwanak-ro, Gwanak-gu, Seoul 08826, Korea

E-mail: [kwang56@snu.ac.kr](mailto:kwang56@snu.ac.kr)

**Keywords:** Eurasian winter cooling, Arctic sea ice loss, Arctic amplification, Arctic oscillation

Supplementary material for this article is available [online](#)

### Abstract

Despite the on-going global warming, recent winters in Eurasian mid-latitudes were much colder than average. In an attempt to better understand the physical characteristics for cold Eurasian winters, major sources of variability in surface air temperature (SAT) are investigated based on cyclostationary EOF analysis. The two leading modes of SAT variability represent the effect of Arctic amplification (AA) and the Arctic oscillation (AO), respectively. These two modes are distinct in terms of the physical characteristics, including surface energy fluxes and tropospheric circulations, and result in significantly different winter SAT patterns over the Eurasian continent. The AA-related SAT anomalies are dipolar with warm Arctic, centered at the Barents–Kara Seas, and cold East Asia. In contrast, the negative AO-related SAT anomalies are characterized by widespread cold anomalies in Northern Eurasia. Relative importance of the AA and the negative AO contributions to cold Eurasian winters is sensitive to the region of interest.

## 1. Introduction

Winters in Eurasian mid-latitudes have been unexpectedly cold in the recent decades (Honda *et al* 2009, Cohen *et al* 2012, Liu *et al* 2012). Several studies suggested that such cold winters might be associated with the negative phase of the North Atlantic oscillation (NAO)/Arctic oscillation (AO) (Francis *et al* 2009, Overland and Wang 2010, Cohen *et al* 2012, Hopsch *et al* 2012, Liu *et al* 2012), and extensive loss of the Arctic sea ice over the Barents–Kara Seas associated with Arctic amplification (AA) (e.g., Mori *et al* 2014). It is not quite clear if AA, AO or sea ice decline act directly on the regional or large-scale circulation leading to the observed cold anomalies. Several studies suggested that these two factors, the AO and the AA, might inherently be related to each other, with the former partly being forced by the latter with a time lag (Liu *et al* 2012, Peings and Magnusdottir 2014). It was then argued that the Arctic sea ice loss in autumn drives a large-scale atmospheric circulation that resembles the negative phase of the NAO/AO in winter; this in turn causes the cold mid-latitudes winter (see the recent reviews by Cohen *et al* (2014) and Vihma (2014)).

The dynamical relationship of the AO and AA, however, is not well established. While many studies agree that the primary impact of the Arctic sea ice loss is in the lower troposphere (Screen and Simmonds 2010a, Stroeve *et al* 2012), the proposed mechanisms by which cold mid-latitude winters are manifested differ significantly and are often unclear.

From a relative short observational record, it is difficult to separate clearly the mechanism operating in the Arctic-induced mid-latitude circulation changes from natural variability. Modeling studies are also not conclusive. Climate model simulations, which are driven by the past sea-ice trends or anomalous sea-ice distribution, yield a wide spectrum of AO response to the Arctic sea ice loss, ranging from a negative phase to a positive one including no outstanding change (Cohen *et al* 2014, Vihma 2014). Likewise, not all models were able to simulate the warm Arctic-cold Eurasia pattern, partly due to an insufficient ensemble size (Mori *et al* 2014, Screen *et al* 2014).

Mori *et al* (2014) recently documented that the AO is distinguishable from the AA. By performing Empirical Orthogonal Function (EOF) analysis over the Eurasian domain, they found that these two modes differ distinctly in their spatial patterns and temporal

evolutions, although the detailed physical mechanisms were not discussed. Based on 100 ensemble simulations of an atmospheric general circulation model, they further separated the AO from the AA as independent contributors to cold winters in Eurasia. This result is quite different from those of earlier studies, which hinted a primary link between Arctic sea ice melting and the NAO/AO.

Earlier studies are still ambiguous in lieu of the connection between the Arctic sea ice change and the development of the AA and AO modes. Moreover, the relative contributions of these two modes to the Eurasian winter surface air temperature (SAT) are not clearly known. In the present study, therefore, Eurasian SAT variability, particularly in winter, is investigated in regard to the AA and AO modes. By extending Mori *et al* (2014), a sophisticated statistical analysis using the cyclostationary EOF (CSEOF) technique is carried out, and the detailed physical characteristics of the AA and AO modes and their role in cold Eurasian winters are examined.

## 2. Data and method of analysis

Data used for this study is the  $1.5^\circ \times 1.5^\circ$  ERA (ECMWF Reanalysis) Interim monthly reanalysis data from 1979 to 2014 (Dee *et al* 2011). Surface and pressure-level (37 levels from 1000 to 1 hPa) variables are analyzed. Sea surface temperature (SST) and sea ice concentration (SIC) data are also from the ERA Interim reanalysis product.

The primary analysis tool is the CSEOF technique (Kim *et al* 1996, Kim and North 1997). In CSEOF analysis, space-time data are decomposed into

$$T(r, t) = \sum_n B_n(r, t) T_n(t), \quad (1)$$

where  $B_n(r, t)$  are cyclostationary loading vectors (CSLV) and  $T_n(t)$  are corresponding principal component (PC) time series. The time-dependent CSLVs are periodic:

$$B(r, t) = B(r, t + d), \quad (2)$$

where  $d$  is called the nested period. The nested period represents the periodicity of underlying covariance statistics (Kim *et al* 2015), which is set to one year in the present study. A primary motivation of CSEOF analysis is to separate distinct physical processes,  $B_n(r, t)$ , together with their stochastic amplitude time series,  $T_n(t)$ .

In order to understand detailed physical mechanisms, several variables should be subject to CSEOF analysis. CSEOF analysis on another variable,  $P(r, t)$ , yields

$$P(r, t) = \sum_n C_n(r, t) P_n(t), \quad (3)$$

where  $C_n(r, t)$  and  $P_n(t)$  are the CSLV and PC time series of  $P(r, t)$ . In general, there is no one-to-one correspondence between  $P_n(t)$  and  $T_n(t)$ , which

implies that  $C_n(r, t)$  and  $B_n(r, t)$  are not physically consistent. We want to write

$$P(r, t) = \sum_n C_n^{(\text{reg})}(r, t) T_n(t), \quad (4)$$

where  $C_n^{(\text{reg})}(r, t)$  is a new CSLV having the amplitude time series  $T_n(t)$ . For this purpose, so-called ‘regression analysis in CSEOF space’ is carried out. This is a two-step procedure:

$$\text{step 1: } T_n(t) = \sum_{m=1}^M \alpha_m^{(n)} P_m(t) + \varepsilon^{(n)}(t), \quad \text{for } n = 1, 2, \dots, \quad (5)$$

$$\text{step 2: } C_n^{(\text{reg})}(r, t) = \sum_{m=1}^M \alpha_m^{(n)} C_m(r, t), \quad \text{for } n = 1, 2, \dots \quad (6)$$

Here  $\{\alpha_m^{(n)}\}$  are regression coefficients and  $\varepsilon^{(n)}(t)$  are regression error time series (see Kim *et al* (2015) for details).

For this study, surface (2 m) air temperature is used as the ‘target’ variable  $T(r, t)$ . Then, CSEOF analysis followed by regression analysis in CSEOF space are carried out on all other variables in order to write the entire data as

$$\text{Data}(r, t) = \sum_n \{B_n(r, t), Z_n^{(\text{reg})}(r, t), U_n^{(\text{reg})}(r, t), V_n^{(\text{reg})}(r, t), \dots\} T_n(t), \quad (7)$$

where the terms in curly braces for each  $n$  represent a physical mechanism derived from individual variables. Each term in curly braces consists of 12 spatial patterns, representing evolution of a physical variable throughout the year. In this way, physically consistent and detailed evolutionary features of a physical mechanism can be investigated. This process, in essence, projects climatological (predictor) variables onto the PC time series of the target variable. Unlike EOF analysis, however, this projection is conducted not in physical space but in CSEOF space.

It should be noted that CSEOF analysis is applied to all months not just to December–January–February (DJF). Furthermore, the whole Northern Hemisphere extratropics north of  $20^\circ$  N is considered instead of the Eurasian domain. These analysis details differ from Mori *et al* (2014) who conducted EOF analysis for the DJF-mean SAT anomalies over the Eurasian domain. To highlight winter season, all results are shown for the boreal winter by averaging the loading vectors in (7) in DJF.

## 3. Results

Figure 1 shows the winter SAT patterns of the two leading CSEOF modes. The first mode, which explains ~15% of the total SAT variability in the Northern Hemisphere extratropics aside from the seasonal cycle, depicts significant warm anomalies in the Arctic region, particularly, over the Barents–Kara Seas, and weak cold anomalies in the East Asian mid-latitudes

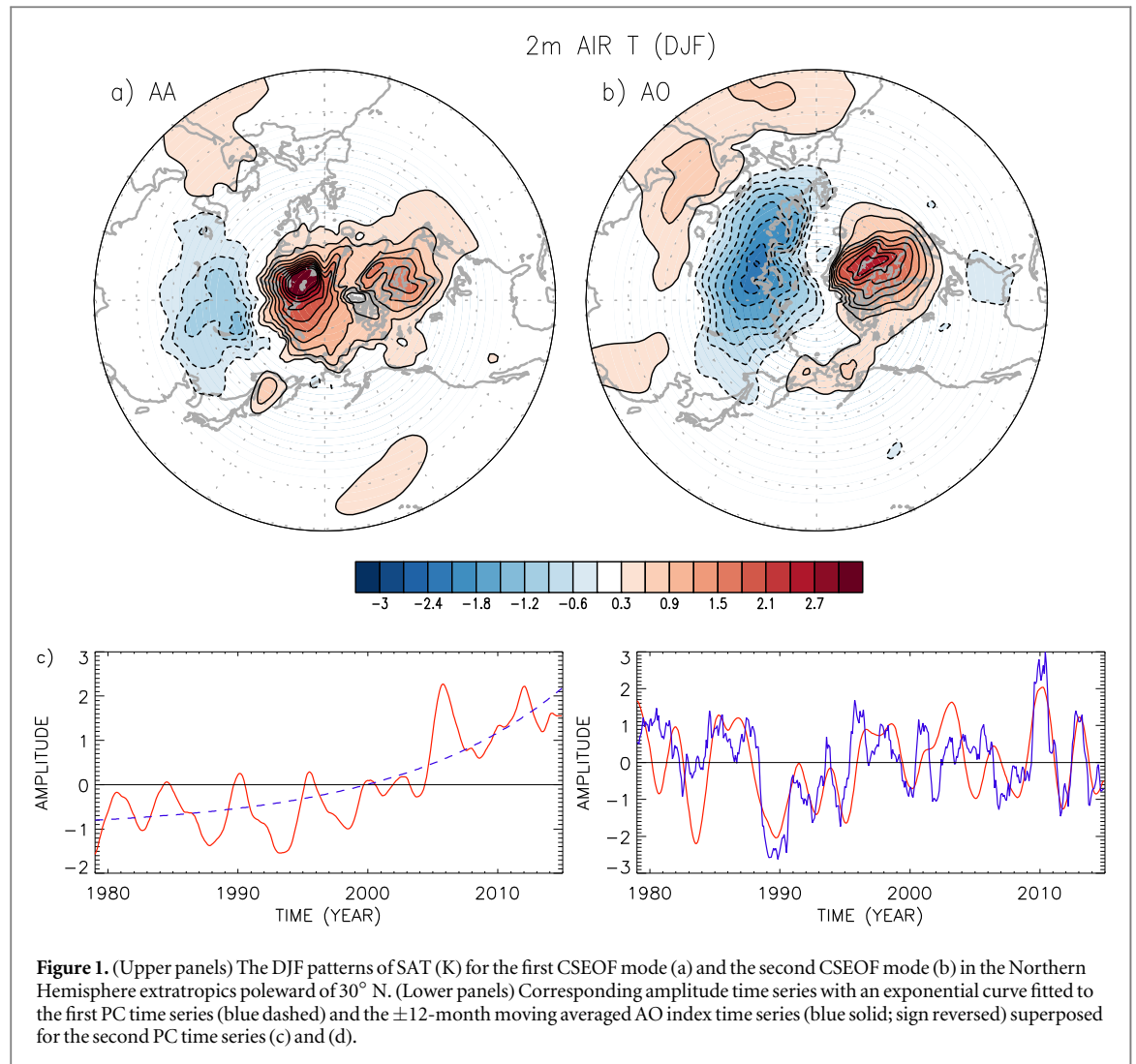
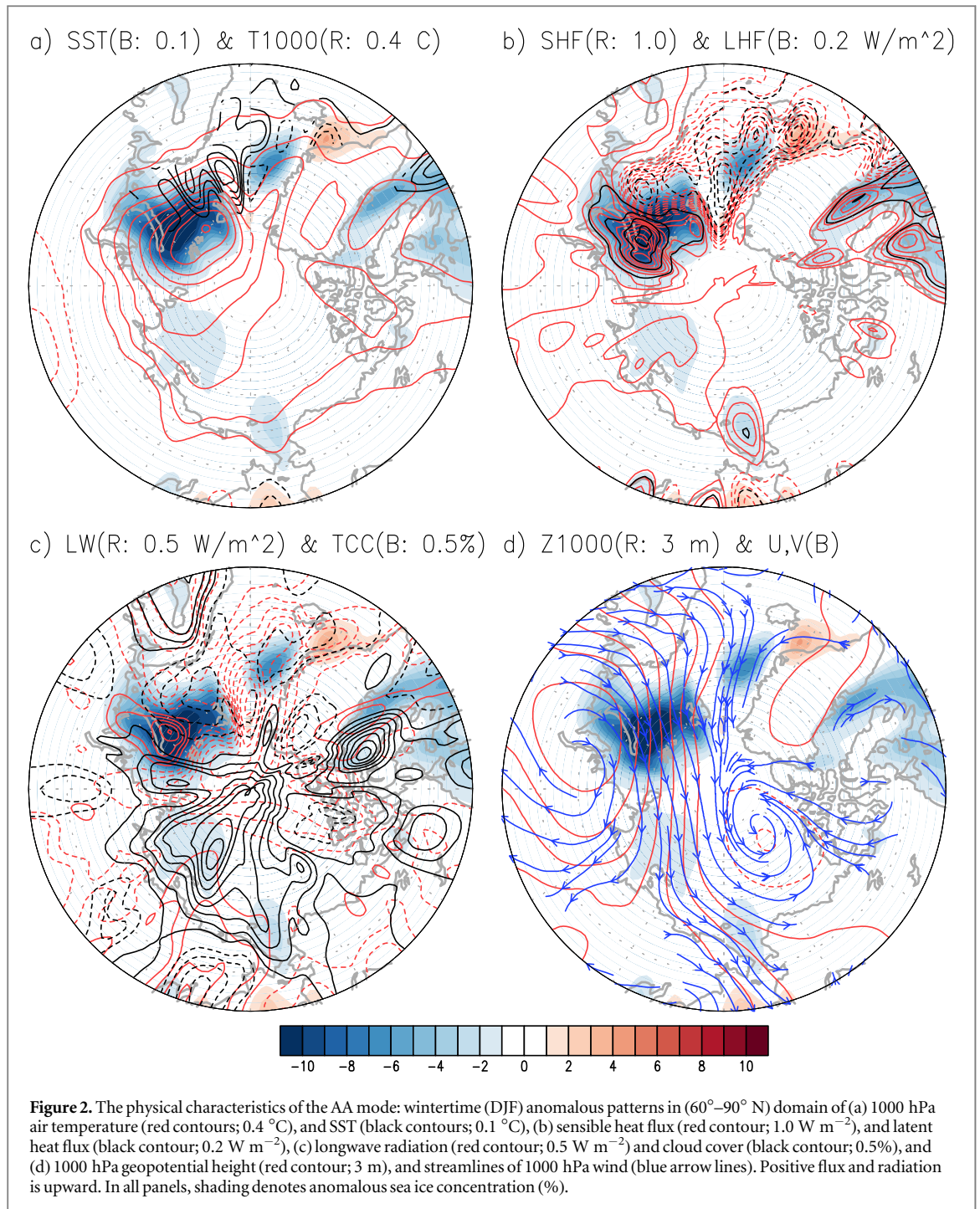


(figure 1(a)). This pattern, which is unique in winter, is often referred to as the warm Arctic-cold Eurasia pattern (Honda *et al* 2009, Overland *et al* 2011, Mori *et al* 2014). During other seasons, such dipolar SAT pattern does not occur and only warm anomalies appear (see figure S1). According to the corresponding amplitude time series, the magnitude of the anomalous SAT pattern increases in an accelerated manner; therefore, this mode is called the AA in the present study.

The second CSEOF mode, explaining  $\sim 8.7\%$  of the total SAT variance, depicts significant warm anomalies over the northern part of North America and North Atlantic and cold anomalies over the northern Eurasia. This SAT pattern is quite similar to that associated with the negative AO (see figure 10 of Thompson and Wallace (2000)). In fact, the corresponding amplitude time series bears a strong resemblance with the  $\pm 12$ -month moving-averaged AO index with a correlation of 0.65 (0.71 with DJF only). Therefore, this mode is called the AO mode in this study (see also figures S2 and S3). The anomalous SAT patterns are most conspicuous in winter (see figure S2). As will be discussed below, the Eurasian SAT

patterns associated with these two leading CSEOF modes bear striking resemblance with those of Mori *et al* (2014).

Physically consistent patterns of sea ice, heat flux, longwave radiation, and 1000 hPa geopotential height/wind for the first and second CSEOF modes are further depicted in figures 2 and 3, respectively. For the AA mode, a significant sea ice loss is seen in the region of anomalously warm SAT (e.g., Barents–Kara Seas). Consistent with this, SST is anomalously warm in the vicinity of sea ice loss, and a significant amount of sensible heat flux and, to a lesser extent, latent heat flux is released from the sea surface exposed to cold air. Previous studies suggest that the increased turbulent heat flux through the exposed sea surface enhances atmospheric warming, which in turn accelerates sea ice melting (Serreze *et al* 2009, Screen and Simmonds 2010a, 2010b). On the other hand, anomalous turbulent heat flux is negative in the North Atlantic, where SIC anomalies are not significant, probably due to the warming of the atmospheric column in association with AA and the decreased temperature contrast between the sea surface and the overlying air. Further, weak net upward longwave

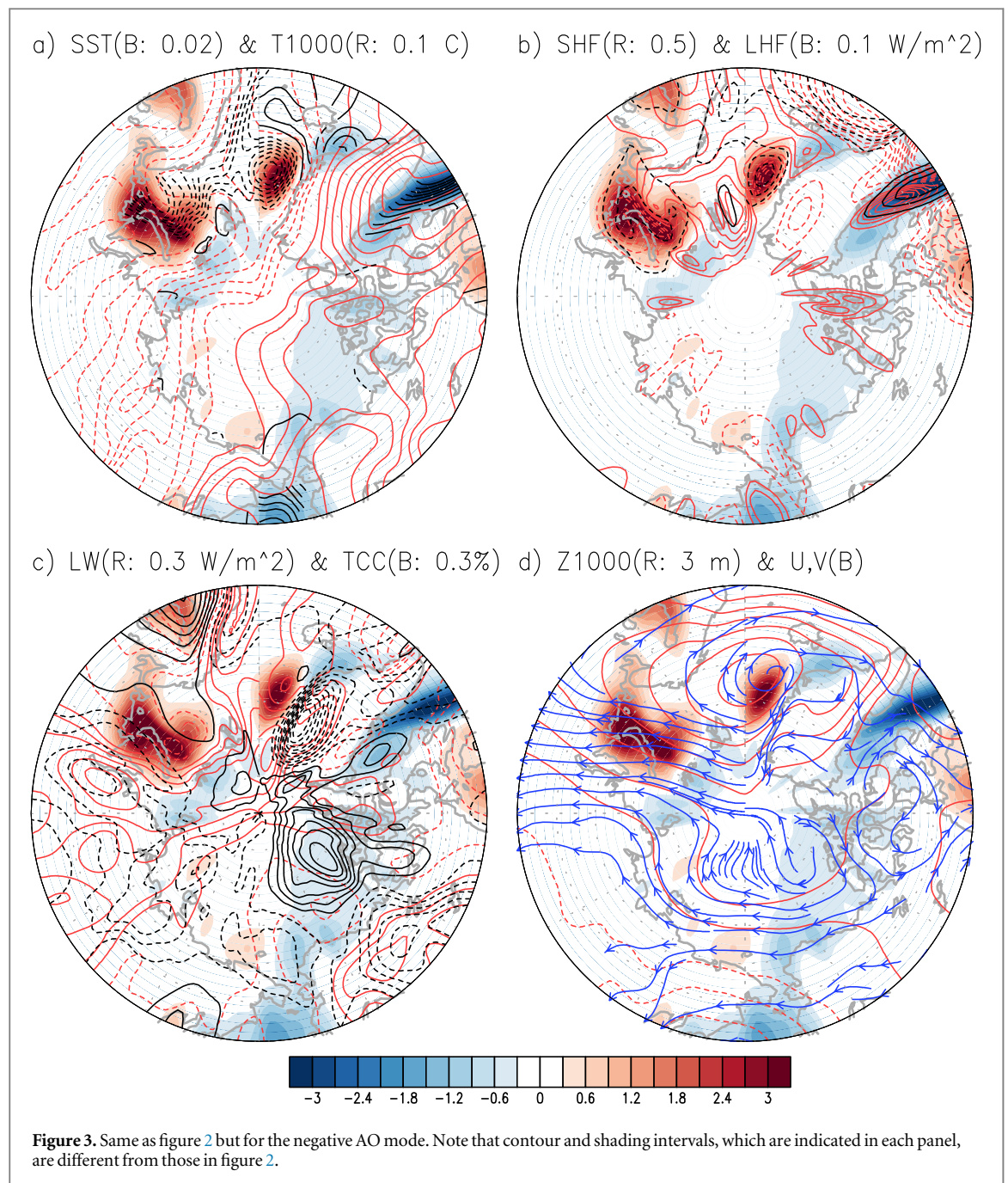


radiation is observed in the reduced SIC region, whereas net downward longwave radiation is significant over the North Atlantic.

The atmospheric circulation associated with the AA mode is characterized by anticyclonic circulation centered at the southeast of the Barents–Kara Seas (figure 2(d)). This circulation pattern, which causes cold temperature advection across East Asia mid-latitudes (figure 1(a)), is due to the lower tropospheric warm anomalies over the region of the Arctic sea ice loss (Serreze *et al* 2009, Screen and Simmonds 2010a, 2010b). The anomalous patterns of geopotential height, temperature and wind are

physically consistent in the context of the hydrostatic and thermal wind balances (see figure S4).

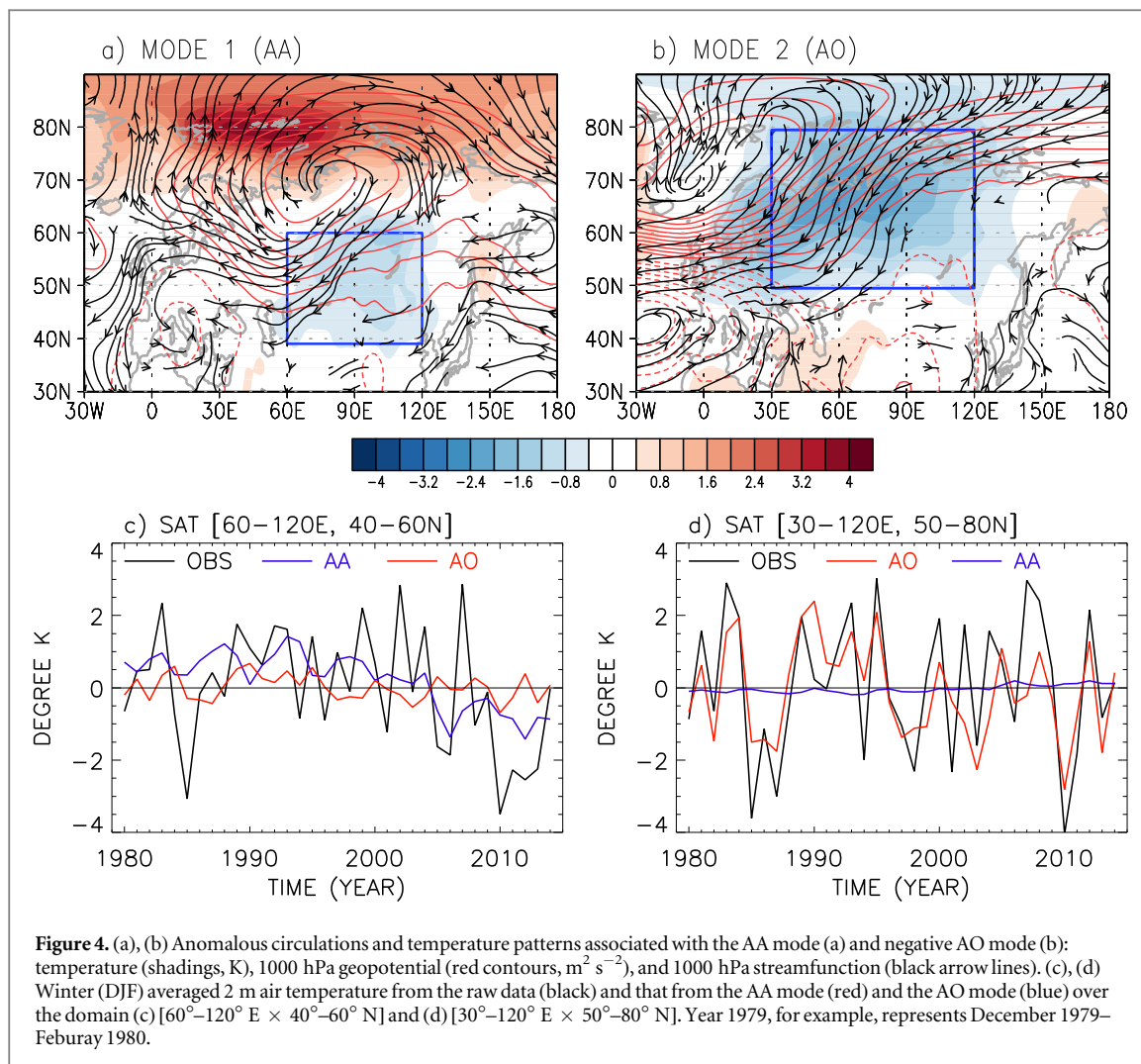
During the negative phase of the AO mode, lower tropospheric temperature is anomalously cold in the eastern half and is anomalously warm in the western half of the Arctic (figure 3(a); see also Thompson and Wallace (2000)). In consistency with SAT anomalies, SIC anomalies are positive over the Barents–Kara Seas and the Greenland Sea, although their changes are only ~1%–3% when the AO index is varied by one standard deviation; this contrasts with a maximum decrease of ~20% when the AA mode is developed (compare figures 2(a) and 3(a)). Sensible and latent



heat flux anomalies in the Arctic are also consistent with SIC and SST anomalies particularly on the eastern side of the North Pacific (figure 3(b)). In general, the sign of net upward longwave radiation is opposite to that of lower tropospheric temperature anomaly, suggesting that upward longwave radiation increases due to anomalously cold tropospheric temperature (figure 3(c)). For the atmospheric circulation, anticyclonic circulation over the Atlantic sector is evident (figure 3(d)). This circulation pattern seems consistent with the sea ice anomaly in the Barents–Kara Seas. The resulting northerly and cold temperature advection explains cold SAT anomalies in the northern part of the Eurasian continent (figure 1(b)). It appears that change in total cloud cover is not significantly

correlated with the sea ice reduction in the Barents–Kara Seas (figures 2(c) and 3(c)). On the other hand, it should be mentioned that the present generation of numerical models does not simulate cloud cover accurately.

It is worthy to note that the AO-related SIC anomalies over the Barents–Kara Seas (figure 3(a)) are somewhat different from what expected from earlier studies. As introduced previously, the negative AO in winter has often been related with the Arctic sea ice loss in autumn (Overland *et al* 2011, Cohen *et al* 2014). Indeed, the AO mode seems to be linked with the sea ice loss in autumn (see figure S6). In winter, however, the negative phase of the AO is related with a slight increase (not decrease) of SIC. It appears that the



decreased SAT over the eastern half of the Arctic in winter during the negative phase of the AO increases SIC particularly over the Barents–Kara Seas. This contrasts to the AA mode which is related with the Arctic sea ice loss in all seasons (see figure S5).

The winter (DJF) patterns of SAT, 1000 hPa geopotential height and stream function anomalies associated with the AA and AO modes are further illustrated in figures 4(a) and (b) for the Eurasian domain. To be consistent with the cold SAT in the mid-latitudes, the negative AO is considered in figure 4(b). The mid-latitude SAT patterns induced by these two modes are again very distinct. One notable difference is the opposite sign of SAT in the Eurasian high-latitudes north of  $\sim 70^\circ$  N. Another striking difference is the center of the anticyclonic circulation. While the AA mode has a circulation center at around [80° E, 70° N], the AO mode has a center at [0°, 75° N]. Because of the opposite SAT anomalies in the Arctic region, the anomalous SIC in the Barents–Kara and Chukchi Seas as well as the associated lower tropospheric change are also opposite in sign between the

AA and the AO modes (see also figures 2 and 3). Further, weak negative SAT anomalies in the AA mode are confined to the region of [60°–120° E × 40°–60° N], whereas those due to the AO mode are widespread in the region of [30°–120° E × 50°–80° N].

Figures 4(a) and (b) clearly indicate that the regions affected by the two CSEOF modes differ substantially, and this difference should be taken into account when examining the Eurasian winter SAT anomalies. Figures 4(c) and (d) show the winter SAT anomaly from 1979/1980 to 2013/2014 averaged over the domains [60°–120° E × 40°–60° N] and [30°–120° E × 50°–80° N], respectively. The SAT variation associated with the AA mode is correlated at 0.50 with the raw winter temperature anomaly averaged over the mid-latitude East Asia and explains  $\sim 25\%$  of the total variance. The AO mode plays a minimal role in this region. On the other hand, the AO mode is correlated at 0.69 with the raw winter temperature anomaly averaged over the high-latitude Eurasia and explains  $\sim 53\%$  of the total variance, while the AA mode explains little of the temperature

variability in this region. This result suggests that the relative importance of the AA and AO modes on Eurasian SAT anomalies is highly sensitive to the region of interest. For example, 2005/06 cold winter in mid-latitude East Asia [ $60^{\circ}$ – $120^{\circ}$  E  $\times$   $40^{\circ}$ – $60^{\circ}$  N] was primarily associated with the AA mode and was not likely linked with the AO mode in any significant manner (figure 4(c)). On the other hand, 2009/10 cold winter over the high-latitude Eurasia [ $30^{\circ}$ – $120^{\circ}$  E  $\times$   $50^{\circ}$ – $80^{\circ}$  N] was likely related with the negative AO mode (figure 4(d)). It should be noted that the AA mode in figure 4(c) explains primarily the long-term trend, whereas the AO mode in figure 4(d) explains the seasonal variability. Thus, the AO is a dominant factor for year-to-year variability while the AA explains the general cooling trend over Eurasia in recent years.

#### 4. Discussion

In this study, the two leading modes of winter SAT variability in the Northern Hemispheric extratropics are identified; i.e., AA mode that is associated with the accelerated warming and sea ice melting in the Arctic region, and AO mode that represents SAT variability associated with the intrinsic (natural) variability. These two modes together explain  $\sim 24\%$  of total SAT variability in the Northern Hemisphere north of  $20^{\circ}$  N. The associated SAT patterns are distinctly different. While the AA mode exhibits a warm Arctic-cold Eurasia pattern, the AO mode shows a widespread monopole pattern with cold Eurasia during its negative phase. Cold Eurasian winters in the recent decades are caused by these two modes, but their relative importance is dependent on the region of interest.

The two leading modes identified in this study are qualitatively similar to those in Mori *et al* (2014). Mori *et al* separated the two leading modes by performing EOF analysis. Their first mode represents the AO, while the second mode resembles the AA mode in the present study; the order of the two modes is switched. This difference is likely results from the methodology. While Mori *et al* used seasonal-mean SAT over the Eurasian domain, monthly-mean SAT anomalies over the whole Northern Hemisphere extratropics, north of  $20^{\circ}$  N, is considered without seasonal averaging in this study.

More importantly, the present study provides the physical characteristics of the AA and AO modes, which were not explored in Mori *et al* (2014). The AA mode is associated with the Arctic sea ice loss, centered at the Barents–Kara Seas, and the enhanced turbulent heat flux from the exposed sea surface. In response to anomalously warm lower troposphere, positive geopotential height anomalies develop to the southeast of the Barents–Kara Seas. This anticyclonic circulation advects cold Arctic air into mid-latitude East Asia,

resulting in cold winters. The negative AO mode, on the other hand, results in anomalously cold SST in the North Atlantic and enhanced SIC in the Barents and Kara Seas. Further, sea ice anomaly related to the AO mode is about an order of magnitude smaller than that associated with the AA mode. Positive geopotential height anomalies develop in the North Atlantic side of the Arctic, leading to anomalous northerly and cold temperature advection in the mid-to-high latitude central Eurasia.

#### Acknowledgments

This research was supported by the Korea Meteorological Administration Research and Development Program under Grant KMIPA 2015-2100 and Korea Ministry of Environment as ‘Climate Change Correspondence Program’. KYK acknowledges support by SNU-Yonsei Research Cooperation Program through Seoul National University in 2015.

#### References

- Cohen J J, Screen A, Furtado J C, Barlow M, Whittleston D, Coumou D, Francis J, Dethloff K, Entekhabi D and Overland J 2014 Recent Arctic amplification and extreme mid-latitude weather *Nat. Geosci.* **7** 627–37
- Cohen J L, Furtado J C, Barlow M, Alexeev V A and Cherry J E 2012 Asymmetric seasonal temperature trends *Geophys. Res. Lett.* **39** L04705
- Dee D, Uppala S, Simmons A, Berrisford P, Poli P, Kobayashi S, Andrae U, Balmaseda M, Balsamo G and Bauer P 2011 The ERA-interim reanalysis: configuration and performance of the data assimilation system *Q. J. R. Meteorol. Soc.* **137** 553–97
- Francis J A, Chan W, Leathers D J, Miller J R and Veron D E 2009 Winter Northern Hemispheric weather patterns remember summer Arctic sea ice extent *Geophys. Res. Lett.* **36** L07503
- Honda M, Inoue J and Yamane S 2009 Influence of low Arctic sea-ice minima on anomalously cold Eurasian winters *Geophys. Res. Lett.* **36** L08707
- Hopsch S, Cohen J and Dethloff K 2012 Analysis of a link between fall Arctic sea ice concentration and atmospheric patterns in the following winter *Tellus A* **64** 18624
- Kim K-Y, Hamlington B and Na H 2015 Theoretical foundation of cyclostationary EOF analysis for geophysical and climatic variables: concepts and examples *Earth-Sci. Rev.* **150** 201–18
- Kim K-Y and North G R 1997 EOFs of harmonizable cyclostationary processes *J. Atmos. Sci.* **54** 2416–27
- Kim K-Y, North G R and Huang J 1996 EOFs of one-dimensional cyclostationary time series: computations, examples, and stochastic modeling *J. Atmos. Sci.* **53** 1007–17
- Liu J, Curry J A, Wang H, Song M and Horton R M 2012 Impact of declining Arctic sea ice on winter snowfall *Proc. Natl Acad. Sci. USA* **109** 4074–9
- Mori M, Watanabe M, Shiogama H, Inoue J and Kimoto M 2014 Robust Arctic sea-ice influence on the frequent Eurasian cold winters in past decades *Nat. Geosci.* **7** 869–73
- Overland J E and Wang M 2010 Large-scale atmospheric circulation changes are associated with the recent loss of Arctic sea ice *Tellus A* **62** 1–9
- Overland J E, Wood K R and Wang M 2011 Warm Arctic-cold continents: climate impacts of the newly open Arctic sea *Polar Res.* **30** 15787



- Peings Y and Magnusdottir G 2014 Response of the wintertime Northern Hemisphere atmospheric circulation to current and projected Arctic sea ice decline: a numerical study with CAM5 *J. Clim.* **27** 244–64
- Screen J A, Deser C, Simmonds I and Tomas R 2014 Atmospheric impacts of Arctic sea-ice loss, 1979–2009: separating forced change from atmospheric internal variability *Clim. Dyn.* **43** 333–44
- Screen J A and Simmonds I 2010a The central role of diminishing sea ice in recent Arctic temperature amplification *Nature* **464** 1334–7
- Screen J A and Simmonds I 2010b Increasing fall-winter energy loss from the Arctic Ocean and its role in Arctic temperature amplification *Geophys. Res. Lett.* **37** L16707
- Serreze M, Barrett A, Stroeve J, Kindig D and Holland M 2009 The emergence of surface-based Arctic amplification *Cryosphere* **3** 11–9
- Stroeve J C, Serreze M C, Holland M M, Kay J E, Malanik J and Barrett A P 2012 The Arctic's rapidly shrinking sea ice cover: a research synthesis *Clim. Change* **110** 1005–27
- Thompson D W J and Wallace J M 2000 Annular modes in the extratropical circulation: I. Month-to-month variability *J. Clim.* **13** 1000–16
- Vihma T 2014 Effects of Arctic sea ice decline on weather and climate: a review *Surv. Geophys.* **35** 1175–214